Since January 2020 Elsevier has created a COVID-19 resource centre with free information in English and Mandarin on the novel coronavirus COVID-19. The COVID-19 resource centre is hosted on Elsevier Connect, the company's public news and information website.

J. Comp. Path. 1986 Vol. 96

PATHOGENESIS OF INFECTIOUS BRONCHITIS NEPHRITIS 1. MORPHOMETRIC ANALYSIS OF KIDNEY PROXIMAL TUBULAR EPITHELIUM IN CHICKENS

By

R. J. Condron* and A. T. Marshall†

*Veterinary Research Institute, Department of Agriculture, Parkville, Victoria 3052, Australia, †Department of Zoology, La Trobe University, Bundoora, Victoria 3083, Australia

INTRODUCTION

It is well documented that infectious bronchitis virus (IBV) produces a nephritis in chickens in natural outbreaks of disease (Winterfield and Hitchner, 1962; Cumming, 1963; Julian and Willis, 1969). Many factors such as cold stress, nutrition, and age and sex of the chicken influence the mortality in an outbreak (Cumming, 1965; Sinkovic and Gilchrist, 1967; Macdonald, Randall and McMartin, 1980). Those strains of virus which induce more severe kidney disease are also associated with higher mortality rates (Siller and Cumming, 1974; Chong and Apostolov, 1982).

In a study of the chemical pathology of infectious bronchitis nephritis, Heath (1970) attributed death of the chicken to kidney dysfunction and acute renal failure. Several histological investigations of the development of kidney lesions through the course of experimental infections have shown interstitial inflammatory reactions and tubular degeneration occurring in both proximal and distal segments of the nephron (Siller and Cumming, 1974; Pohl, 1974; Purcell, Tham and Surman, 1976).

Chong and Apostolov (1982), by immuno-fluoresence, demonstrated the presence of viral antigen in all segments of tubules, but the staining was mainly confined to the proximal tubules. These workers incriminated the replication of the virus in the tubular epithelium as a direct cause of the disease.

This paper presents a quantitative morphological analysis of the changes in structure of the proximal tubular epithelial cells over the course of an experimental infection with IBV.

MATERIALS AND METHODS

Experimental Birds

Sixteen 3-week-old specific-pathogen-free (SPF) Webster-Mini crossbred chickens were supplied by the Commonwealth Scientific and Industrial Research Organization, Animal Health Division. Regular monitoring and serological testing have shown the birds from this isolation unit to be free from a wide range of mycoplasma, bacteria and viruses.

0021–9975/86/010047 + 16 $03.00/0

Virus

The "T" strain of IBV (Winterfield, Cumming and Hitchner, 1964) was obtained from Dr T. Faragher, National Biological Standards Laboratory, Parkville, Victoria. The virus was passaged once in embryonated (SPF) eggs and the allantoic fluid, harvested at day 12, was stored in 1 ml aliquots at −70 °C. In subsequent egg inoculation studies' the titre of IBV was found to be 3×10^4 EID_{50} per ml.

Plan of Experiment

Birds were placed in a controlled temperature room at 12 °C to induce cold stress. After 3 days, 4 control birds were anaesthetized and the left kidney was perfused with fixative via the renal portal vein. The remaining birds were inoculated with 10 µl of the viral suspension into both conjunctival sacs. At 4 day intervals thereafter, kidneys were fixed from groups of 4 birds.

Tissue Processing

Kidneys were perfused for at least 3 min under 90 cm hydrostatic pressure with a fixative consisting of 1·5 per cent glutaraldehyde, 1 per cent formaldehyde and 1·2 per cent glucose in 0·1 M cacodylate buffer. Osmotic pressure of the buffer and glucose was 265 mOs per kg and the fixative was 540 mOs per kg. The pH was 7·4. The renal vein was sectioned and the portal valve was clamped. Acceptable perfusion was indicated if the kidney became pale and turgid. The kidney was then immediately removed from the bird, cut into 1 mm slices and placed in the same fixative for 1 h at 0 °C. Tissue was washed in buffer 3 times and post-fixed in 1 per cent osmium tetroxide for 1 h, block stained with 2 per cent aqueous uranyl acetate for 1 h, dehydrated and embedded in Spurr's firm resin (Spurr, 1969). Specimens for sectioning were selected at random and the criteria for adequate fixation were that the lumens of the proximal tubules were open, the microvilli were regularly arranged and the apical border of the cell was straight, with no protrusion into the lumen (Maunsbach, 1966a). Silver sections 60 to 90 nm thick, from 3 blocks per bird, were collected on grids and stained with 0·3 per cent lead citrate for 3 min.

For scanning electron microscopy (SEM) slices of fixed tissue were processed by the OTO method (Kelley, Dekker and Bluemink, 1975) and dried by the critical point method in CO_2. The specimens were fractured, mounted on aluminium stubs and coated with 20 nm of gold.

Electron Microscopy

Transmission electron micrographs were taken of cells in longitudinal section (extending from the basement membrane to the lumen) from 6 different proximal tubules per section with a JEOL JEM–120. A magnification of 3600 was used for investigation of whole cells and 25 000 for detailed investigation of microvilli and organelles in the apical and basal parts of the cell. The magnification of the microscope was confirmed with a 1200 lines per mm diffraction grating replica. A JEOL JSM–T20 was used at 5 kV to take scanning electron micrographs.

Stereology

Micrographs were printed with a further magnification of 3·6 and analysed with a microcomputer with a graphics tablet and an image analysis programme*. Data were collected from the digitizing tablet by tracing the outline of individual structures with a cursor for whole cell, nucleus, microvillus and extracellular space at low magnification level. At the high magnification, the following structures were analysed within a reference area overlay arbitrarily placed over the micrographs; microvillus membrane,

* Scientific Microprograms, 213 Merwin Road, Raleigh, NC 27606 U.S.A.

apical tubular membrane, apical vacuoles, lysosomes, apical and basal mitochondria cristal and inner mitochondria membrane, lipid droplets and basolateral membrane.

Stereological characteristics were calculated from standard formulae (Weibel, 1963; Williams, 1977). Formfactor is the ratio, $4\pi \times$ area divided by $(\text{perimeter})^2$ which gives an estimate of shape of structures. This ratio is 1·0 for a perfect circle. Nucleus profile diameter was calculated by taking the square root of the product of the diameters measured at right angles. By assuming that the nucleus was spherical, Fullman's formula (Williams, 1977 was applied to determine the mean nucleus diameter. The absolute volumes of the cell and cell components were then extrapolated from the nucleus volume and the relative volume densities.

The sample size required to achieve results with confidence limits of ± 10 per cent was determined from a study of normal chicken kidney (Condron, unpublished data). All values used in this investigation were measured from a large number of micrographs from 3 chickens. Progressive means were determined by including each additional observation. As a range of ± 10 per cent of the final overall mean is considered adequate accuracy in biological studies, the sample size, or number of observations, needed to bring the progressive mean constantly into this range is the minimal sample required to obtain a valid estimate of a particular measurement (Burri, Giger, Gnagi and Weibel, 1968; Weibel and Gnagi, 1968; Schroeder and Munzel-Pedrazzoli, 1970; Williams, 1977). To increase the significance of the results the minimal sample size was exceeded with an extra animal in experimental groups, as this type of sampling has greater statistical weight than increasing the number of micrographs examined from a smaller group.

The systematic subsampling employed has been shown to be a valid method of obtaining a representative unbiased measurement for morphometric analysis of a polarized tissue (Burri *et al.*, 1968; Schroeder and Munzel-Pedrazzoli, 1970). In order to determine the trend of the results through the course of the disease, statistical analysis for linear and quadratic regression against time was performed by applying the *t*-test to orthogonal polynomials (Hicks, 1973). A further statistical comparison between groups was by the one-way analysis of variance.

RESULTS

All birds exhibited typical signs of infectious bronchitis. From day 3 onwards, the birds had ruffled feathers and were depressed. These signs were most severe between days 7 to 10 and some birds passed very fluid droppings. At day 8, the kidneys were swollen and pale, and urates were observed in the ureters. The disease produced was "mild" in character (Siller and Cumming, 1974) and no natural deaths occurred. Examination by light microscopy revealed a predominantly mononuclear inflammatory response.

Quantitative morphological data for cellular components at the low magnification are given in Tables 1 to 3. Volume densities of the nucleus, microvillus and extracellular space relative to the total cell volume are given in Table 1. Compared with the normal "control" group, the nucleus volume density tended to be reduced but this was not significant. The microvillus volume density was reduced at days 4, 8 and 12 and showed a linear regression; the extracellular space volume density was reduced at days 4 and 8 and returned to normal at day 12 with a quadratic regression. The values calculated for the absolute volume of these structures, shown in Table 2, followed this same pattern. The reduction of microvillus volume was due to shortening and focal loss of microvilli.

TABLE 1

VOLUME DENSITY AS A PERCENTAGE OF CELLULAR COMPONENTS RELATED TO THE TOTAL VOLUME OF PROXIMAL TUBULAR EPITHELIAL CELLS (MEAN ± S.E.M.)

	Control	*Day 4*	*Day 8*	*Day 12*	P *value*
Nucleus	13·7 ± 0·90	12·1 ± 0·55	12·8 ± 0·90	12·6 ± 0·98	N.S.
Microvillus	12·1 ± 1·06	11·1 ± 0·65	10·1 ± 0·09	10·0 ± 0·53	< 0·05†
Extracellular	10·5 ± 0·21	9·2 ± 0·12	9·2 ± 0·37	10·5 ± 0·48	< 0·02*‡

Statistical analysis, *P* value, N.S. = not significant.
* = Analysis of variance.
† = Orthogonal polynomial, linear effect.
‡ = Orthogonal polynomial, quadratic effect.

TABLE 2

ABSOLUTE VOLUME(μm^3) OF CELLULAR COMPONENTS (MEAN ± S.E.M.)

	Control	*Day 4*	*Day 8*	*Day 12*	P *value*
Cell	826 ± 77	803 ± 49	776 ± 59	862 ± 89	N.S.
Nucleus	115 ± 16	98 ± 10	101 ± 18	106 ± 4	N.S.
Microvillus	97 ± 5	89 ± 6	78 ± 9	87 ± 10	N.S.
Extracellular space	87 ± 9	73 ± 4	72 ± 10	90 ± 10	< 0·1‡
Cytoplasm	527 ± 50	543 ± 32	525 ± 52	580 ± 67	N.S.

Statistical analysis, *P* value, N.S. = not significant.
‡ = Orthogonal polynomial, quadratic effect.

Estimators of cell and nucleus shapes are listed in Table 3. There was an increase in cell formfactor at day 4 and an increase in cell maximal diameter at day 8, indicating that initially the cells became rounder and then decreased in size and became more elongated, returning to normal dimensions at day 12. The nuclear diameter remained relatively constant but there was an increase in formfactor at day 8. This rounding-up of the nucleus occurred later than similar changes in the cell.

The surface density or surface area per unit volume of membrane structures is presented in Table 4. There was a marked reduction in apical tubular membrane at day 4. This returned to normal at day 8, giving a significant quadratic regression against the shorter time interval. The relative density of microvillus membrane remained constant but the surface density per cell was reduced as the microvillus volume density decreased. Similarly, the slight increase in relative density of the basolateral membrane was overshadowed by a decrease in extracellular space, so that there was an overall decrease in the absolute surface areas of transport membranes per cell.

Table 5 lists the volume densities of cytoplasmic components. After an initial reduction, there was an increase in apical vacuoles at day 8 and a progressive increase in lysosomes in the apical cytoplasm over the course of the experiment. However, these values were not significant in the statistical tests applied due to large variations between animals. A large increase in lipid droplets was observed in the base of the cells at day 4 but they were normal by day 8.

There was a marked change in the distribution and shape of mitochondria. In the apical cytoplasm, there was an increase of mitochondria volume density at day 4, a decrease at day 8 and normal values at day 12. In the base of the cell, there was a decrease in mitochondria volume density which was most severe at day 8. These changes in volume density reflect changes in size and shape of individual mitochondrial profiles observed (Table 6). In the apical cytoplasm, with increase in volume density at day 4, the mitochondria had larger profiles which were longer and had more distorted or less rounded shapes. The subsequent decrease in volume density was accompanied by shorter, more rounded and smaller profiles towards day 12. In the basal cytoplasm, the decrease in volume density was mirrored by a decrease in size of individual profiles. The mitochondria became shorter and rounder towards day 12. The measurements related to shape were the same for apical and basal profiles at day 12. The inner mitochondrial membrane plus the cristal membrane had constant surface density per unit volume of mitochondria, but since there was a decrease in mitochondrial volume density there was a related decrease in mitochondrial membrane per cell.

Figure 1 shows a typical epithelial cell from a normal chicken taken at low magnification. At day 4 (Fig. 2), the cells tended to be more rounded. There was a decrease in apical tubular membrane and an increase in apical mitochondrial volume density. Lipid droplets were prominent at the base of the cell. Virus particles could be found in cells at day 4 (Fig. 3). They were enclosed within irregular spaces adjacent to the nucleus by a membrane from which virus particles were budding.

Figure 4 shows an epithelial cell at day 8 with focal loss of microvilli. There

TABLE 3
ESTIMATORS DESCRIBING CELL AND NUCLEUS SHAPE (MEAN ± S.E.M.)

	Control	*Day 4*	*Day 8*	*Day 12*	P *value*
Cell formfactor	0·695 ± 0·008	0·730 ± 0·015	0·694 ± 0·015	0·681 ± 0·006	<0·1* <0·05‡
Cell profile max diam (μm)	14·4 ± 0·30	14·5 ± 0·33	15·3 ± 0·33	15·0 ± 0·14	<0·1†
Nucleus formfactor	0·876 ± 0·011	0·904 ± 0·018	0·928 ± 0·019	0·895 ± 0·017	<0·1‡
Nucleus profile max diam (μm)	4·73 ± 0·16	4·61 ± 0·10	4·83 ± 0·13	4·76 ± 0·06	N.S.
Nucleus diameter (μm)	5·98 ± 0·31	5·70 ± 0·19	5·72 ± 0.34	5.86 ± 0·07	N.S.

Statistical analysis, *P* value, N.S. = not significant.
* = Analysis of variance.
† = Orthogonal polynomial, linear effect.
‡ = Orthogonal polynomial, quadratic effect.

TABLE 4
SURFACE DENSITY OF MEMBRANE STRUCTURES PER UNIT VOLUME OF CELLULAR COMPONENT AND PER UNIT OF CELL VOLUME (μm^2 PER μm^3) AND TOTAL MEMBRANE AREA PER CELL (μm^2) (MEAN ± S.E.M.)

	Control	*Day 4*	*Day 8*	*Day 12*	P *value*
Surface density					
Apical tubular memb. per ap cytoplasm	10·02 ± 0·98	7.68 ± 0·31	10·01 ± 0·83	8·92 ± 0·76	<0·1ø
Microvillus memb. per microvillus	25·2 ± 0·90	25·8 ± 0·30	25·5 ± 1·1	24·6 ± 0·45	N.S.
Basolateral memb. per extracellular space	16·1 ± 0·40	16·8 ± 1·02	17·7 ± 0·91	15·3 ± 0·44	<0·1‡
Microvillus memb. per cell	3·04 ± 0·23	2·86 ± 0·14	2·57 ± 0·11	2·46 ± 0·15	<0·05†
Basolateral memb. per cell	1·69 ± 0·06	1·54 ± 0·09	1·62 ± 0·24	1·61 ± 0·08	N.S.
Total area					
Microvillus memb. per cell	2466 ± 226	2313 ± 149	2008 ± 273	2135 ± 272	N.S.
Basolateral memb. per cell	1407 ± 167	1237 ± 142	1261 ± 158	1329 ± 193	N.S.
Total memb. per cell	3873 ± 319	3550 ± 248	3269 ± 423	3776 ± 282	N.S.

Statistical analysis, *P* value, N.S. = not significant.
† = Orthogonal polynomial, linear effect.
‡ = Orthogonal polynomial, quadratic effect.
ø = Orthogonal polynomial, quadratic effect to Day 8.

TABLE 5
VOLUME DENSITY AS A PERCENTAGE OF UNIT OF APICAL OR BASAL CYTOPLASM (MEAN ± S.E.M.)

	Control	*Day 4*	*Day 8*	*Day 12*	P *value*
Apical vacuoles	5·3 ± 0·81	4·5 ± 2·04	7·7 ± 2·07	5·8 ± 1·46	N.S.
Apical lysosomes	0·6 ± 0·35	1·1 ± 1·13	1·4 ± 0·62	2·0 ± 0·18	N.S.
Apical mitochondria	17·1 ± 2·26	25·7 ± 1·94	13·3 ± 2·64	16·5 ± 2·32	<0·05*‡
Basal mitochondria	56·0 ± 1·08	50·3 ± 1·67	48·9 ± 2·23	50·8 ± 0·98	<0·05*†‡
Basal lipid droplets	0·9 ± 0·86	3·5 ± 1·10	0·9 ± 0·31	1·2 ± 0·50	<0·1*

Statistical analysis, *P* value, N.S. = not significant.
* = Analysis of variance.
† = Orthogonal polynomial, linear effect.
‡ = Orthogonal polynomial, quadratic effect.

TABLE 6
ESTIMATES OF VARIABLES DESCRIBING APICAL AND BASAL MITOCHONDRIA (MEAN ± S.E.M.)

		Control	*Day 4*	*Day 8*	*Day 12*	P *value*
Surface density of inner and cristal membrane relative to mitochondria volume (μm^2 per μm^3)	Apical	22·3 ± 0·80	22·0 ± 0·48	20·7 ± 1·15	20·7 ± 0·66	N.S.
	Basal	21·3 ± 0·47	20·8 ± 0·26	20·2 ± 0·46	20·7 ± 0·63	N.S.
Formfactor	Apical	0·837 ± 0·012	0·773 ± 0·034	0·753 ± 0·032	0·830 ± 0·023	<0·1*<0·05‡
	Basal	0·801 ± 0·010	0·797 ± 0·021	0·767 ± 0·038	0·831 ± 0·006	N.S.
Profile max diam (μm)	Apical	0·565 ± 0·032	0·692 ± 0·048	0·649 ± 0·027	0·551 ± 0·049	<0·1*<0·02‡
	Basal	0·681 ± 0·010	0·645 ± 0·021	0·644 ± 0·069	0·553 ± 0·018	<0·05†
Profile area (μm^2)	Apical	0·140 ± 0·009	0·173 ± 0·008	0·141 ± 0·005	0·120 ± 0·016	<0·1†<0·05*‡
	Basal	0·177 ± 0·006	0·160 ± 0·004	0·148 ± 0·021	0·122 ± 0·006	<0·05*<0·01†

Statistical analysis, *P* value, N.S. = not significant.
* = Analysis of variance.
† = Orthogonal polynomial, linear effect.
‡ = Orthogonal polynomial, quadratic effect.

was also a reduction in apical mitochondria. At day 12 (Figs 7 and 8), mitochondria were dark and cristae were dilated. Figure 7 shows a cell with marked loss of microvilli. Vesicular spaces were prominent between cells (Fig. 8). These spaces or "holes" in the cells were obvious in scanning electron micrographs (Figs 9 and 10).

Cytoplasmic inclusions into nuclei were observed at days 4, 8 and 12 (Fig. 5). Figure 6 shows a leucocyte migrating through the basement membrane and between two epithelial cells. This was common at days 8 and 12. Figures 11 and 12 show the basal part of the cell at the high magnification from a normal chicken and from a chicken at 12 days after infection, respectively. At 12 days, the mitochondria were smaller and more rounded, the mitochondrial matrix was condensed and the cristae were dilated. The endoplasmic reticulum was dilated.

DISCUSSION

Although the disease reproduced in this study was mild, viral replication and kidney disease were observed and the chickens were obviously sick and depressed. The size of the infective dose, route of administration and increased egg passage are factors which are potential causes of the decreased virulence of this "T" strain of IBV compared to that reported by Siller and Cumming (1974).

Throughout the course of the disease, significant alterations in the structure of the functional components within the proximal tubular epithelium were observed. In particular, there was a decrease in the volume density of mitochondria and in the surface area of membrane structures. Both the microvillus membrane adjacent to the tubular lumen and the basolateral membrane adjacent to the extracellular space, which are separated by tight junctions at the apex of the cell, were reduced. The membrane available for transport of fluid and ions across the cell was thus decreased. Within the cell, there was also a reduction in apical tubular membrane which is associated with uptake of larger molecules (Siller, 1971).

Fig. 1. Proximal tubular epithelial (PTE) cell from a normal (control) chicken. Tubular lumen (TL), Microvilli (M), Apical tubular apparatus (AT), Apical vacuoles (AV), Villous processes of basolateral membrane in extracellular space (B) and Vascular sinus (V). × 4500.

Fig. 2. PTE cell from a chicken 4 days after infection with IBV. Lipid droplets (L). × 5000.

Fig. 3. Virus particles (arrow) budding into an irregular membrane bound space. × 47 500.

Fig. 4. PTE cell 8 days after infection with IBV. Focal loss of microvilli and decrease in mitochondria. × 6500.

Fig. 5. PTE cell 4 days after infection with IBV. Cytoplasmic inclusion into the nucleus (CI), erythrocyte (E) in vascular sinus. × 7800.

Fig. 6. Migration of a leucocyte (L) through the basement membrane (arrow) into the extracellular space between two epithelial cells at 8 days post-infection with IBV. Endothelial lining (EL) of vascular sinus. × 7200.

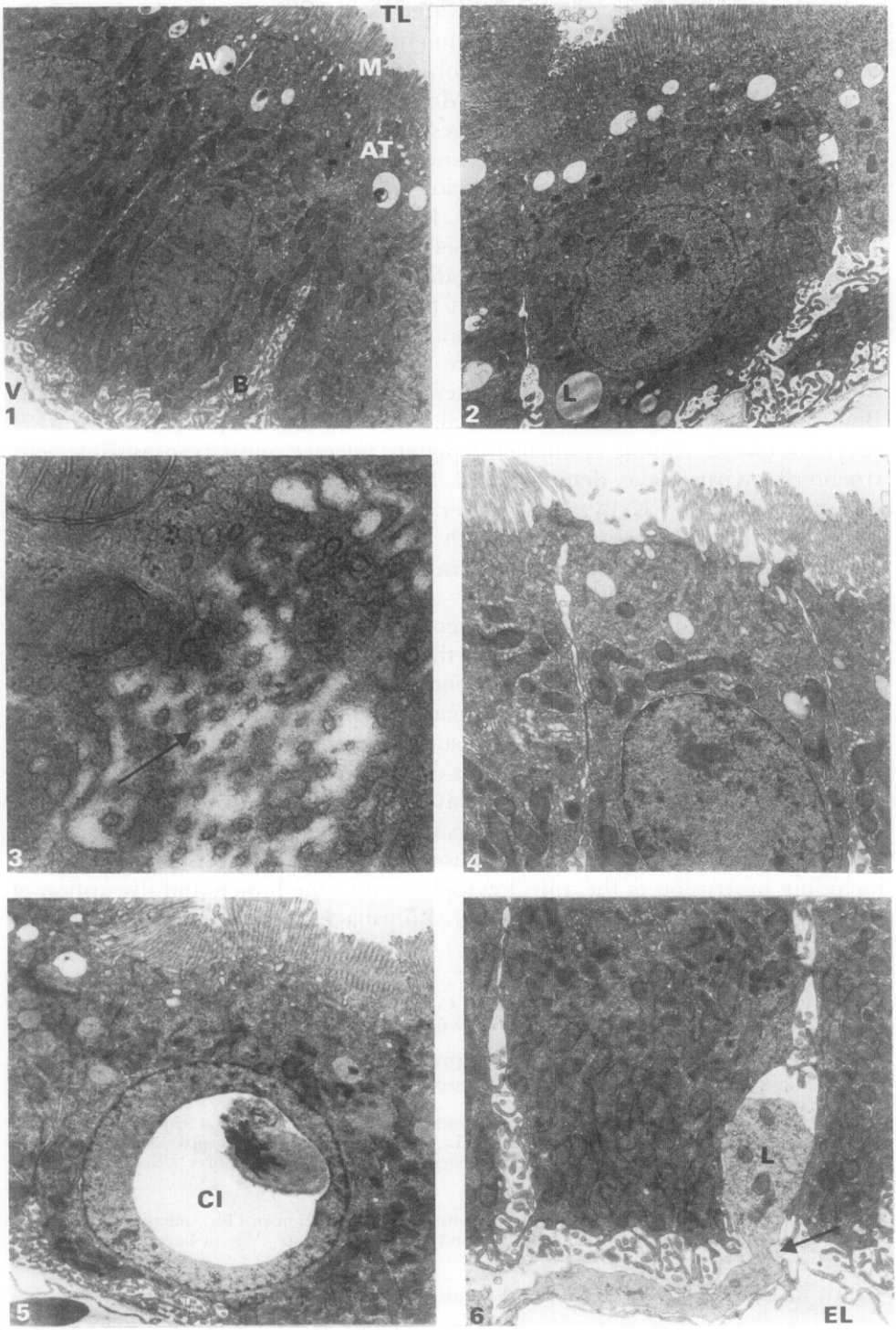
TL
AV
M
AT
V
B
1
2
L
3
4
CI
5
L
6
EL

Further evidence for change in water and ion transport is the dilated endoplasmic reticulum and the alteration in mitochondrial size and shape. The severity and degree of the changes observed correspond to stages 2 and 3 described by Trump, Croker and Mergner (1971) in their review of the pathogenesis of cell injury. These stages are compatible with cell survival but indicate a modification of cell membrane function and/or a modification of cell energy metabolism. There is a very close relationship between structure and function in membranes (Trump *et al.*, 1971). In studies of acute renal failure induced by ischaemia in rats, it has been shown that cells with these changes have ineffective ion and volume regulation. Glaumann, Glaumann, Berezesky and Trump (1975) concluded that, at this stage, sodium reabsorption by the proximal tubule must be greatly impaired.

Similar alterations in the structure of cells have also been described in animals infected by coronaviruses other than IBV (Cheville, 1975; Takeuchi, Binn, Jervis, Keenan, Hildebrandt, Valas and Bland, 1976). Measurements in short-circulated jejunal epithelia of piglets infected with transmissible gastroenteritis virus have demonstrated abnormal glucose-stimulated sodium transport (Kerzner, Kelly, Gall, Butler and Hamilton, 1977). These workers associated this impaired function with the presence of abnormal, immature villous epithelial cells which have migrated to the villi in a relatively undifferentiated state.

Although there have been many recent advances in the determination of the replication strategy of coronaviruses, the mechanism of viral release has still not been clearly defined (Robb and Bond, 1979; Siddell, Wege and ter Meulen, 1982). Evidence for cell lysis as the means of viral release has frequently been presented from studies in which the tissues have not received optimal preservation. Adequate preservation of tissue is essential to minimize fixation artefacts. Lysis and rupture of cells was not a feature of this study in which tissues were perfused with a carefully monitored fixative. Immersion fixation is unsuitable since rapid collapse of the tissue causes damage to the tubular epithelium including protrusion of the apical cytoplasm into the lumen and disruption of the microvillus border of the cells (Maunsbach, 1966a; Rothwell, 1974).

Fig. 7. PTE cell 12 days after infection with IBV. Condensation of mitochondrial matrix with dilation of cristae and considerable loss of microvilli. × 6500.

Fig. 8. PTE cell 12 days after infection with IBV. Vesicular spaces are seen between cells (VS). Mitochondria are dark and cristae are dilated. × 6500.

Fig. 9. SEM of a proximal tubule fractured longitudinally between cells, from a chicken 12 days after infection with IBV. Tubular lumen (TL), Microvilli (M), Villous processes of basolateral membrane (B), Vascular sinus (V), Erythrocyte (E) and Vesicular structures (VS) in lateral surface of cells. × 2200.

Fig. 10. SEM of PTE cell 12 days after infection with IBV. Tubular lumen (TL), microvilli (M), villous processes of basolateral membrane (B) and vesicular structure (VS) in lateral surface of cells. × 6600.

Fig. 11. Basal part of PTE cell from a normal (control) chicken. × 47 500.

Fig. 12. Basal part of PTE cell 12 days after infection with IBV. There is condensation of mitochondrial matrix with dilatation of cristae and dilated endoplasmic reticulum. × 47 500.

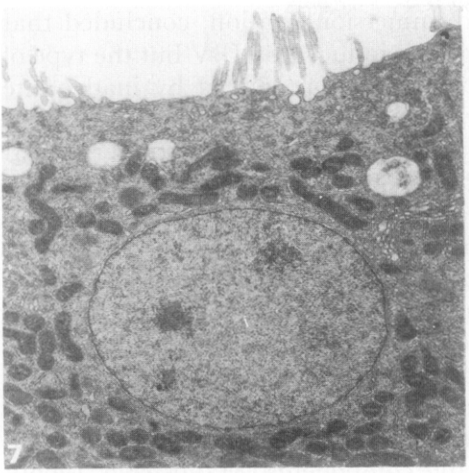

7

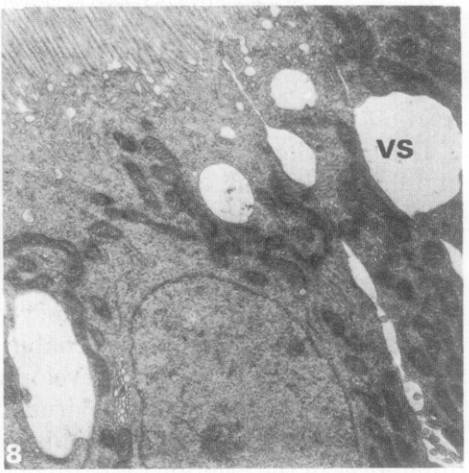

8

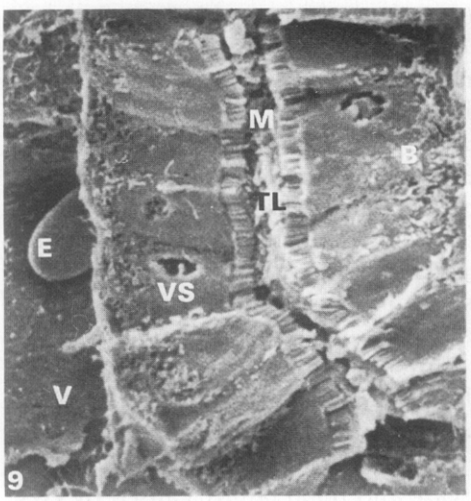

9

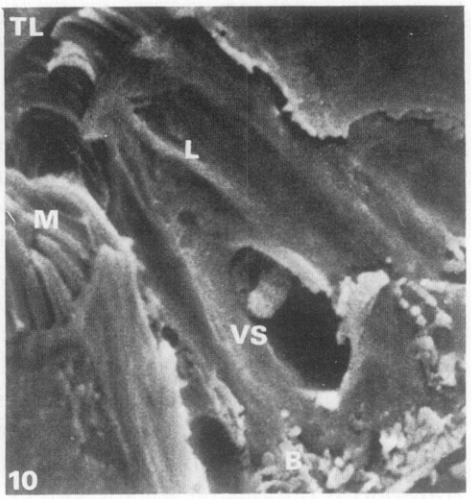

10

11

12

Chong and Apostolov (1982), who used immersion fixation, concluded that lysis of cells was the primary cause of nephritis induced by IBV but the type of lysis of cells which they observed may be readily produced by inadequate fixation.

Doughri, Storz, Hajer and Fernando (1976), Chasey and Alexander (1976) and Bielefeldt-Ohmann and Bloch (1982) have presented evidence that release of coronavirus may occur by fusion of viral-containing cytoplasmic vacuoles with the plasma membrane. Vesicular, hole-like structures in the lateral surfaces of cells which were observed by SEM are possibly the site of viral release by this mechanism of exocytosis. Release of virus by this means and survival of the infected cell to enable the further maturation of viral particles may play some part in the development of persistent infections which have been reported for some coronaviruses including IBV (Robb and Bond, 1979).

The proximal tubular epithelium has been shown to be very sensitive to differences in the osmotic pressure of fixative components (Maunsbach, 1966b; Rothwell, 1978). Alterations in the concentrations of ions and hence of osmotic pressure initiated by IBV infection will cause changes in the osmotic differential of a fixative which is kept constant. Some of the observed changes in structure may have been related to this osmotic effect of the fixative. With more concentrated solutions, Maunsbach (1966b) observed widened extracellular spaces similar to the spaces observed at day 12, but further evidence that this is an osmotic effect, such as shrunken nuclei and densly staining cytoplasm, is lacking. These widened spaces may be related to the vesicular structures observed by SEM. Permeability of infected cells to trypan blue (Robb and Bond, 1979) may be due to these "holes" in the plasma membrane.

Although the primary virus-cell interaction in coronavirus-caused disease is a cytocidal interaction, general cellular protein synthesis is not affected until very late in the infectious cycle (Robb and Bond, 1979). The evidence presented in our study of structural alterations in tubular epithelial cells during the course of IBV infection indicates that impaired fluid and electrolyte transport is responsible for the kidney disease and renal failure caused by IBV. Further work (Condron and Marshall, 1985) is in progress to determine the alteration in the function of the proximal tubular epithelium and to relate it to the structural changes described in this paper.

Whilst stereological methods have been used in a wide range of EM investigations of experimental pathology, to the authors' knowledge, this is the first report of a morphometric analysis of ultrastructural changes in an organ induced by a viral infection. These techniques, designed to define the extent and nature of structural changes in all cells in a particular organ, can play a valuable rôle in determining virus-host cell interactions and the pathogenesis of viral diseases.

SUMMARY

The ultrastructure of the proximal tubular epithelial cells in chicken kidneys was examined throughout the course of an experimental infection with

infectious bronchitis virus. A quantitative assessment of the structural changes in the cells was related to these in normal cells.

Significant alterations were detected in the membrane structures and in the mitochondria. There was a reduction in surface area of the microvillus membrane, the basolateral membrane and the apical tubular membrane. There were alterations in the shape of mitochondrial profiles and a decrease in the volume density of mitochondria. Vesicular structures, which are a possible site of viral release, were observed in the lateral surface of cells.

These changes in the functional components of the cells indicate impaired transport of ions and water. The results demonstrate the value of stereological methods for the study of viral-host cell interactions in the pathogenesis of viral disease.

ACKNOWLEDGMENTS

This work was carried out as partial fulfillment of the degree of PhD at La Trobe University by R.J.C. and was supported by a grant to A.T.M. from the Australian Research Grants Scheme. The Veterinary Research Institute received financial assistance from the Victorian Chicken Meat Council towards S.P.F. facilities.

The authors are grateful to Professor J.S. Maritz, Mathematics Department (Statistics), La Trobe University, for advice on the statistical analysis of the results.

REFERENCES

Bielefeldt-Ohmann, H., and Bloch, B. (1982). Electron microscopic studies of bovine viral diarrhoea virus in tissues of diseased calves and in cell cultures. *Archives of Virology*, **71,** 57–74.

Burri, P. H., Giger, H., Gnagi, H. R., and Weibel, E. R. (1968). Application of stereological methods to cytophysiologic experiments on polarised cells. *Proceedings of 4th European Conference for Electron Microscopy (Rome)*, **1,** 593–594.

Chasey, D., and Alexander, D. J. (1976). Morphogenesis of avian infectious bronchitis virus in primary chick kidney cells. *Archives of Virology*, **52,** 101–111.

Cheville, N. F. (1975). Cytopathology in viral diseases, Coronaviruses. *Monographs in Virology*, **10,** 150–157.

Chong, K. T., and Apostolov, K. (1982). The pathogenesis of nephritis in chickens induced by infectious bronchitis virus. *Journal of Comparative Pathology*, **92,** 199–211.

Condron, R. J., and Marshall, A. T. (1985). Pathogenesis of infectious bronchitis nephritis. 2. Studies of water and electrolyte balance in colostomised chickens. *Avian Pathology*, (in press).

Cumming, R. B. (1963). Infectious avian nephrosis (uraemia) in Australia. *Australian Veterinary Journal*, **39,** 145–147.

Cumming, R. B. (1965). The present position of infectious bronchitis in Australia. *Proceedings of 3rd World Poultry Association Congress (Paris)*, pp. 141–144.

Doughri, A. M., Storz, J., Hajer, I., and Fernando, H. S. (1976). Morphology and morphogenesis of a coronavirus infecting intestinal epithelial cells of newborn calves. *Experimental and Molecular Pathology*, **25,** 355–370.

Glaumann, B., Glaumann, H., Berezesky, I. K., and Trump, B. F. (1975). Studies on the pathogenesis of ischaemic cell injury. *Virchows Archives B Cell Pathology*, **19,** 281–302.

Heath, B. C. (1970). Chemical pathology of nephrosis induced by an infectious bronchitis virus. *Avian Diseases*, **14,** 95–106.

Hicks, C. R. (1973). *Fundamental Concepts in the Design of Experiments.* 2nd Edit. Holt, Rinehart and Winston, New York.

Julian, R. J., and Willis, N. G. (1969). The nephrosis-nephritis syndrome in chickens caused by a Holte strain of infectious bronchitis virus. *Canadian Veterinary Journal,* **10,** 18–19.

Kelley, R. O., Dekker, R. A. F., and Bluemink, J. G. (1975). In *Principles and Techniques of Scanning Electron Microscopy,* Volume 4. M. A. Hayat, Ed., Van Nostrand Reinhold, New York, pp. 34–44.

Kerzner, M. B., Kelly, M. H., Gall, M. D., Butler, D. G., and Hamilton, J. R. (1977). Transmissible gastroenteritis: sodium transport and the intestinal epithelium during the course of viral enteritis. *Gastroenterology,* **72,** 457–461.

Macdonald, J. W., Randall, C. J., and McMartin, D. A. (1980). An inverse age resistance of chicken kidneys to infectious bronchitis virus. *Avian Pathology,* **9,** 245–259.

Maunsbach, A. B. (1966a). The influence of different fixatives and fixation methods on the ultrastructure of rat kidney proximal tubule cells. *Journal of Ultrastructure Research,* **15,** 242–282.

Maunsbach, A. B. (1966b). The influence of different fixatives and fixation methods on the ultrastructure of rat kidney proximal tubule cells. *Journal of Ultrastructure Research,* **15,** 283–309.

Pohl, R. (1974). The histopathogenesis of the nephrosis-nephritis syndrome. *Avian Pathology,* **3,** 1–13.

Purcell, D. A., Tham, V. L., and Surman, P. G. (1976). The histopathology of infectious bronchitis in fowls infected with a nephrotropic T strain of virus. *Australian Veterinary Journal,* **52,** 85–91.

Robb, J. A., and Bond, C. W. (1979). Coronaviridae. *Comprehensive Virology,* **14,** 193–247.

Rothwell, B. (1974). Perfusion fixation of the kidney of the domestic fowl. *Journal of Microscopy,* **100,** 99–104.

Rothwell, B. (1978). The use of osmolality as an aid to establishing consistent fixation quality: studies on the kidney of the domestic fowl. *British Poultry Science,* **19,** 213–218.

Schroeder, H. E., and Munzle-Pedrazzoli, S. (1970). Application of stereologic methods to stratified gingival epithelia. *Journal of Microscopy,* **92,** 179–198.

Siddell, S., Wege, H., and ter Meulen, V. (1982). The structure and replication of coronaviruses. *Current Topics in Microbiology and Immunology,* **99,** 131–163.

Siller, W. G. (1971). Structure of the kidney. In *Physiology and Biochemistry of the Domestic Fowl,* D. N. Bell and B. M. Freeman, Eds, Academic Press, London, pp. 197–231.

Siller, W. G., and Cumming, R. B. (1974). The histopathology of an interstitial nephritis in the fowl produced experimentally with infectious bronchitis virus. *Journal of Pathology,* **114,** 163–173.

Sinkovic, B., and Gilchrist, P. (1967). The effect of nutrition, environment and sex on the mortality from infectious bronchitis uraemia. *Proceedings of Australian Poultry Science Convention,* pp. 35–43.

Spurr, A. R. (1969). A low-viscosity epoxy resin embedding medium for electron microscopy. *Journal of Ultrastructure Research,* **26,** 31–43.

Takeuchi, A., Binn, L. N., Jervis, H. R., Keenan, K. P., Hildebrandt, P. K., Valas, R. B., and Bland, F. F. (1976). Electron microscope study of experimental enteric infection in neonatal dogs with a canine coronavirus. *Laboratory Investigation,* **34,** 539–549.

Trump, B. F., Croker, B. P., and Mergner, W. J. (1971). The role of energy metabolism ion and water shifts in the pathogenesis of cell injury. In *Cell Membranes, Biological and Pathological Aspects,* G. W. Richter, D. G. Scarpelli and N. Kaufman, Eds, Williams & Wilkins Co., Baltimore, pp. 84–128.

Weibel, E. R. (1963). Principles and methods for the morphometric study of the lung and other organs. *Laboratory Investigation,* **12,** 131–155.

Weibel, E. R., and Gnagi, H.R. (1968). Improvements in efficiency of stereologic methods in electron microscopic cytology. *Proceedings of 4th European Conference for Electron Microscopy (Rome)*, **1,** 601–602.

Williams, M. A. (1977). Stereological techniques. In *Practical Methods in Electron Microscopy*, Volume 6, Pt. 2, A. M. Glauert, Ed., North Holland, Amsterdam, pp. 1–84.

Winterfield, R. W., Cumming, R. B., and Hitchner, S. B. (1964). Serological study of Australian chickens affected with a uremia disease syndrome. *Avian Diseases,* **8,** 234–244.

Winterfield, R. W., and Hitchner, S. B. (1962). Etiology of an infectious nephritis-nephrosis syndrome of chickens. *American Journal of Veterinary Research,* **23,** 1273–1278.

[*Received for publication, August 25th,* 1984]